

## Metal Substitution in Keggin-Type Tridecameric Aluminum–Oxo–Hydroxy Clusters

Wallace O'Neil Parker, Jr.,\* Roberto Millini, and Imre Kiricsi†

Department of Physical Chemistry, Eniricerche S.p.A., 20097 San Donato (MI), Italy

Received May 29, 1996<sup>⊗</sup>

The species resulting from a typical preparation for metal-substituted hybrids of the Keggin tridecamer,  $\text{Al}_{13}$  or  $[\text{AlO}_4\text{Al}_{12}(\text{OH})_{24}(\text{OH}_2)_{12}]^{7+}$ , were examined by performing  $^{27}\text{Al}$  NMR on the solutions during aging and by studying the precipitated sulfate salts via solid state  $^{27}\text{Al}$  NMR and powder X-ray diffraction (XRD). Aqueous mixtures (0.25 mol  $\text{L}^{-1}$ ) of  $\text{AlCl}_3$  and another metal ion (M), in a 12:1 mole ratio (Al:M), where  $\text{M} = \text{Fe}^{3+}$ ,  $\text{Zn}^{2+}$ ,  $\text{Ga}^{3+}$ ,  $\text{In}^{3+}$ ,  $\text{Sn}^{2+}$ ,  $\text{La}^{3+}$ , and  $\text{Bi}^{3+}$ , were subjected to forced hydrolysis by addition of  $\text{NaOH}$  (1.0 mol  $\text{L}^{-1}$ ) until  $\text{OH}/(\text{Al} + \text{M}) = 2.25$ , and the kinetics of  $\text{Al}_{13}$  formation and disappearance with aging at 80 °C was monitored by  $^{27}\text{Al}$  NMR spectroscopy.  $\text{Al}_{13}$  units polymerize on aging with an apparent rate constant ( $k$ ) of  $4.8(8) \times 10^{-2} \text{ h}^{-1}$  to form a species referred to as  $\text{AlP}_2$ . Only the solutions containing  $\text{Ga}^{3+}$  and  $\text{Sn}^{2+}$  exhibited faster  $\text{Al}_{13}$  conversion rates.  $\text{GaAl}_{12}$  forms quickly at 80 °C ( $k = 0.54 \text{ h}^{-1}$ ) and is more stable than  $\text{AlP}_2$ .  $\text{Sn}^{2+}$  apparently promotes  $\text{AlP}_2$  formation ( $k = 0.38 \text{ h}^{-1}$ ). XRD and solid state NMR reveal that only the Ga hybrid can be prepared by this method. No hybrid formation was evidenced using  $\text{M} = \text{Mg}^{2+}$ ,  $\text{Fe}^{3+}$ ,  $\text{Co}^{2+}$ ,  $\text{Ni}^{2+}$ ,  $\text{Cu}^{2+}$ ,  $\text{Zn}^{2+}$ ,  $\text{In}^{3+}$ ,  $\text{La}^{3+}$ , or  $\text{Ce}^{3+}$  at 25 °C or  $\text{M} = \text{Co}^{2+}$  or  $\text{La}^{3+}$  under reflux conditions. Isostructural (cubic symmetry) single crystals were obtained for the sulfate salts of  $\text{Al}_{13}$  and  $\text{GaAl}_{12}$ . Single-crystal XRD analysis of these two polyoxocations provides the first rigorous comparison between them and shows they have very similar structures. The main crystallographic data for  $\text{Al}_{13}$  and  $\text{GaAl}_{12}$  are as follows:  $\text{Na}[\text{AlO}_4\text{Al}_{12}(\text{OH})_{24}(\text{H}_2\text{O})_{12}](\text{SO}_4)_4 \cdot 10\text{H}_2\text{O}$ , cubic,  $F43m$ ,  $a = 17.856(2)$  Å,  $Z = 4$ ;  $\text{Na}[\text{GaO}_4\text{Al}_{12}(\text{OH})_{24}(\text{H}_2\text{O})_{12}](\text{SO}_4)_4 \cdot 10\text{H}_2\text{O}$ , cubic,  $F43m$ ,  $a = 17.869(3)$  Å,  $Z = 4$ . Thus, the greater thermal stability of  $\text{GaAl}_{12}$  cannot be rationalized in terms of the overall geometric considerations, as suggested by others. Solid state NMR also shows the coordination symmetries of the outer 12 Al nuclei in both clusters to be similar.

## Introduction

Recently, great interest has developed for the Keggin-type aluminum polyoxocation  $[\text{AlO}_4\text{Al}_{12}(\text{OH})_{24}(\text{H}_2\text{O})_{12}]^{7+}$ , hereafter referred to as  $\text{Al}_{13}$ , as a pillaring agent to produce PILCs (pillar interlayered clays).<sup>1</sup> Due to its low thermal stability,  $\text{Al}_{13}$  is not an ideal pillar since industrially used PILC catalysts need frequent regeneration.

Poor thermal stability has been suggested to correlate with cluster structure.<sup>2,3</sup>  $\text{Al}_{13}$  has a central Al atom surrounded by twelve edge-sharing ( $\text{AlO}_6$ ) octahedra. The central tetrahedral Al atom is smaller than the cavity formed by the outer Al nuclei. Thermal stability might be increased by substituting the central Al atom with a larger metal atom to reduce the distortions of the surrounding octahedra (we will refer to these isomorphously substituted polyoxocations as Keggin hybrids). The incorporation of many different metal ions ( $\text{M} = \text{La}^{3+}$ ,  $\text{Mg}^{2+}$ , and all the transition metals) into the Keggin ion has been claimed. Usually there is no distinction between which type of Al substitution occurs (tetrahedral or octahedral). In our view, convincing physical evidence for  $\text{MAl}_{12}$  hybrids has been reported only in the case of  $\text{Ga}^{3+}$ .<sup>2–5</sup> The reports of  $\text{V}^{3+}$  ions,<sup>6</sup>

$\text{Fe}^{3+}$ ,<sup>7–9</sup>  $\text{Re}^{3+}$  ions,<sup>10</sup>  $\text{La}^{3+}$ ,<sup>11</sup> and the transition M in general<sup>12</sup> are based on chemical rather than structural analyses. Workers generally characterize the PILCs rather than the pillars.

Typical substitution schemes involve thermal treatments of aqueous solutions of the mixed metal salts under hydrolysis conditions. Even without substitution,  $\text{Al}_{13}$  is converted to other (more thermally stable) species. This means that in many PILC syntheses,  $\text{Al}_{13}$  is a minor species or totally absent.<sup>13–15</sup> Usually it is the hydrolyzed analog of  $\text{Al}_{13}$  that serves as the initial pillaring agent.<sup>16</sup> Recently, Nazar and co-workers<sup>17,18</sup> identified the initial thermal decomposition product of  $\text{Al}_{13}$  as  $\text{AlP}_2$ , thought to be formed by condensation of two Keggin ions that have each lost a monomer ( $\text{Al}_{24}\text{O}_{72}$ ). This higher molecular

\* Present address: Jozsef Attila Univ., H-6720 Szeged, Rerrich B.t. 1, Hungary.

<sup>⊗</sup> Abstract published in *Advance ACS Abstracts*, January 15, 1997.

- (1) Vaughan, D. E. W.; Lussier, R.; Magee, J. S. U.S. Pat. 4 176 090, 1978.
- (2) Bradley, S. M.; Kydd, R. A.; Fyfe, C. A. *Inorg. Chem.* **1992**, *31*, 1181.
- (3) Bradley, S. M.; Kydd, R. A.; Yamdagni, R.; Fyfe, C. A. In *Expanded Clays and Other Microporous Solids*; Ocelli, M. L.; Robson, H. E., Eds.; Van Nostrand Reinhold: New York, 1992; Vol. II, p 13.
- (4) Gorz, H.; Schonherr, S.; Pertlik, F. *Monatsh. Chem.* **1991**, *122*, 759.
- (5) (a) Bradley, S. M.; Kydd, R. A.; Yamdagni, R. *J. Chem. Soc., Dalton Trans.* **1990**, 413. (b) Coelho, A. V.; Poncelet, G. *Appl. Catal.* **1991**, *77*, 303. (c) Thomas, B.; Goertz, H.; Schonherr, S. *Z. Chem.* **1987**, *27*, 183.
- (6) Attalla, M. I.; Bruce, L. A.; Hoggson, S. I.; Turney, T. W.; Wilson, M. A.; Batta, B. D. *Fuel* **1990**, *69*, 725.

- (7) Bergaya, F.; Hassoun, N.; Barrault, J.; Gatineau, L. *Clay Miner.* **1993**, *28*, 109.
- (8) (a) Bergaya, F.; Hassoun, N.; Gatineau, L.; Barrault, J. In *Preparation of Catalysts 5*; Poncelet, G., et al., Eds.; Elsevier: Amsterdam, 1991; p 329. (b) Lee, W. Y.; Raythatha, R. H.; Tartarchuk, B. J. *J. Catal.* **1989**, *115*, 159. (c) Skoularikis, N. D.; Coughlin, R. W.; Kostapapas, A.; Carrado, K.; Suid, S. L. *Appl. Catal.* **1988**, *39*, 61.
- (9) Zhao, D.; Wang, G.; Young, Y.; Guo, X.; Wang, Q.; Ren, J. *Clay Miner.* **1993**, *41*, 317.
- (10) (a) Mc Cauley, J. R. Int. Pat. Appl. PCT/US88/00567, 1988. (b) Trillo, J. M.; Alba, M. D.; Castro, M. A.; Poyato, J.; Tobias, M. M. *J. Mater. Sci.* **1993**, *28*, 373. (c) Sterte, J. In *Preparation of Catalysts 5*; Poncelet, G., et al., Eds.; Elsevier: Amsterdam, 1991; p 301. (d) Brindley, G. W.; Yamanaka, S. *Am. Mineral.* **1979**, *64*, 830.
- (11) Zhao, D.; Yang, Y.; Guo, X. *Mater. Res. Bull.* **1993**, *28*, 939.
- (12) Vaughan, D. E. W., et al. U.S. Patent 4 248 739 and 4 666 877.
- (13) Akitt, J. W. *Prog. Nucl. Magn. Reson. Spectrosc.* **1989**, *21*, 1.
- (14) Wang, W.-Z.; Hsu, P. H. *Clay Miner.* **1994**, *42*, 356.
- (15) Schoonhedyt, R. A.; Eynde, J.; Tubbax, H.; Leeman, H.; Stuyckens, M.; Lenotte, L.; Stone, W. E. *Clay Miner.* **1993**, *41*, 598.
- (16) Pinnavaia, T. J.; Landau, S. D.; Tzou, M.-S.; Johnson, I. D. *J. Am. Chem. Soc.* **1985**, *107*, 7222.
- (17) Fu, G.; Nazar, L. F.; Bain, A. D. *Chem. Mater.* **1991**, *3*, 602.
- (18) Nazar, L. F.; Fu, G.; Bain, A. D. *J. Chem. Soc., Chem. Commun.* **1992**, 251.
- (19) Sterte, J. *Catal. Today* **1988**, *2*, 219 and references therein.
- (20) Tokarz, M.; Shabtai, J. *Clay Miner.* **1985**, *33*, 89.

weight species (referred to as AIP<sub>2</sub>) provides PILCs that are more hydrothermally stable than those pillared with Al<sub>13</sub>.<sup>19,20</sup>

The lack of physical–chemical evidence for the M–Al Keggin hybrids claimed in the literature prompted us to propose an indirect solution state <sup>27</sup>Al NMR method for indicating if isomorphous substitution occurs.<sup>21a</sup> Hydrolysis (OH/Al = 2.25) of 0.25 mol L<sup>-1</sup> AlCl<sub>3</sub> solutions at 80 °C provided convenient conditions for following the transformations, as Al<sup>3+</sup> is converted to Al<sub>13</sub> and then to AIP<sub>2</sub>. Unfortunately, direct methods for verifying M–Al hybrids via NMR of the M nuclei (many being paramagnetic) are not practical. Recently, we investigated the incorporation of Fe<sup>3+</sup> and Cr<sup>3+</sup> ions using Mossbauer and <sup>27</sup>Al NMR spectroscopy and concluded that no isomorphous substitution occurs in the tetrahedral or octahedral positions of Al<sub>13</sub> Keggin ions.<sup>21b–e</sup> Here, the solution state NMR method is combined with the direct solid state analysis of the precipitated products (powder XRD and <sup>27</sup>Al NMR) to verify if M–Al Keggin hybrids more stable than Al<sub>13</sub> (or AIP<sub>2</sub>) are formed. PILC stability is dependent on the stability of the pillaring agent.<sup>22,23</sup> Thus, only metal polyoxocations with greater stability than Al<sub>13</sub> are of interest. This report accounts a multidisciplinary search for these M–Al cations using the most commonly cited M in the literature.

We must stress the following. There is no doubt that mixed oxide pillared clays, as synthesized using literature methods, can exhibit excellent catalytic properties. However, there is considerable doubt about the isomorphous substitutions of different metal ions into the Al<sub>13</sub> Keggin ions.

## Experimental Section

Partial forced hydrolysis, with 1.0 mol L<sup>-1</sup> NaOH, of the aqueous metal halide solutions (initially 0.25 mol L<sup>-1</sup>) was performed at 25 °C as previously reported.<sup>21a</sup> The 80 °C aged solutions (ca. 1 L) were kept in volumetric flasks in an oven, and 2 mL aliquots were withdrawn at predetermined intervals. These solutions were studied by NMR (at 25 °C where hydrolysis is very slow) within 1 h. The sulfate salts were prepared by adding 0.1 mol L<sup>-1</sup> Na<sub>2</sub>SO<sub>4</sub> to the cooled solution of aged Keggin ions. The pH was maintained at 4.5 by addition of dilute H<sub>2</sub>SO<sub>4</sub>. After a few days, the crystals formed were filtered and dried in air.

<sup>27</sup>Al (78.2 MHz), <sup>71</sup>Ga (91.5 MHz), and <sup>139</sup>La (42.4 MHz) NMR spectra were obtained on a Bruker CXP-300 spectrometer. Solution state spectra were made at 25 °C as previously reported.<sup>21a</sup> Chemical shifts are referenced externally to aqueous solutions (1.0 mol L<sup>-1</sup>) of AlCl<sub>3</sub> and GaCl<sub>3</sub> (both 0 ppm) and La(NO<sub>3</sub>)<sub>3</sub> (2.7 mol L<sup>-1</sup>, -8.5 ppm). Solid state <sup>27</sup>Al NMR spectra were collected on samples contained in 7 mm zirconia rotors using 0.4 μs (π/10) rf pulses and a 2 s recycle delay. MAS (magic angle spinning) spectra are shown in the power mode to give all positive signals.

X-ray powder diffraction (XRD) patterns were collected on a computer-controlled Phillips PW1710 vertical diffractometer equipped with a pulse–height analyzer, variable divergence slits, and a monochromator on the diffracted beam. Data were collected stepwise in the appropriate angular region, using Cu Kα (λ = 1.541 78 Å). Before elaboration, data were converted to fixed divergence slit of 1°.

**Single-Crystal X-ray Data Collection and Structure Refinement.** Single-crystal X-ray diffraction analyses were performed on a Siemens AED diffractometer, using Mo Kα radiation (λ = 0.710 69 Å). Unit cell dimensions and the crystal orientation matrix were determined by

a least-squares fit of the setting angles of 30 strong reflections collected in the range 12 ≤ θ ≤ 17°. Intensity data were collected with the θ/2θ method, with θ<sub>max</sub> = 35°. One intense reflection was monitored for every 50 reflections collected. Data were corrected for Lorentz and polarization effects. The main crystallographic data are provided in Table 4. The structural model adopted for the refinement of the structures of Al<sub>13</sub> and GaAl<sub>12</sub> sulfate salts is that reported by Goerz et al.<sup>4</sup> Refinements were performed anisotropically for all the non-H atoms (48 parameters) with the SHELX-76 computer program.<sup>24</sup> Geometrical data were computed with the program PARST.<sup>25</sup>

**Na[AlO<sub>4</sub>Al<sub>12</sub>(OH)<sub>24</sub>(H<sub>2</sub>O)<sub>12</sub>](SO<sub>4</sub>)<sub>4</sub>·10H<sub>2</sub>O (Al<sub>13</sub>).** A colorless regular tetrahedral crystal with an edge dimension of 0.30 mm was used for data collection and structure refinement. A total of 3415 reflections were measured, of which 669 were unique and 454 with *F* > 4σ(*F*) were considered observed. The (008) reflection, monitored every 50 reflections, showed a 3% intensity decay after total collection. The refinement was performed by considering the cubic *F* $\bar{4}3m$  space group. A total of 53 parameters, including positional and anisotropic thermal parameters for all non-hydrogen atoms, were refined using full-matrix least-squares techniques. Refinement converged at *R* = 0.058 and *R*<sub>w</sub> = 0.064, with *w* = 1/[σ<sup>2</sup>(*F*) + 0.004737*F*<sup>2</sup>].

**Na[GaO<sub>4</sub>Al<sub>12</sub>(OH)<sub>24</sub>(H<sub>2</sub>O)<sub>12</sub>](SO<sub>4</sub>)<sub>4</sub>·10H<sub>2</sub>O (GaAl<sub>12</sub>).** A colorless regular tetrahedral crystal with an edge dimension of 0.25 mm was used for data collection and structure refinement. A total of 3444 reflections were measured, of which 672 were unique and 467 with *F* > 4σ(*F*) were considered observed. The (222) reflection, monitored every 50 reflections, showed no intensity decay after total collection. The refinement was performed by considering the cubic *F* $\bar{4}3m$  space group. A total of 53 parameters, including positional and anisotropic thermal parameters for all non-hydrogen atoms, were refined using full-matrix least-squares techniques. Refinement converged at *R* = 0.055 and *R*<sub>w</sub> = 0.059, with *w* = 1/[σ<sup>2</sup>(*F*) + 0.006064*F*<sup>2</sup>].

## Results and Discussion

<sup>27</sup>Al NMR studies of aluminum clusters have one major drawback. At lower field strengths, some aluminum nuclei may not be detected. Al nuclei having large quadrupole coupling constants (QCC), as a result of low coordination symmetries, can give signals broadened beyond detection.<sup>13</sup> In the solution state <sup>27</sup>Al NMR experiments made here with OH/(Al + M) = 2.25, ca. 60% of the signal area is missing, based on an unhydrolyzed AlCl<sub>3</sub> reference solution. A large portion of this NMR-silent Al is part of alumina sol. Solid state <sup>27</sup>Al NMR detects nuclei with high QCCs provided that sufficiently large magnetic field strengths are used. A 14 T field strength, double the one used here, is needed to observe signals for <sup>27</sup>Al nuclei with QCC = 10.5 MHz,<sup>26</sup> which are representative of some nuclei in this study.

**Attempted Synthesis of Al<sub>13</sub> Hybrids at 25 °C.** Initially, the preparation of M–Al hybrids was attempted under mild conditions (OH/(Al + M) = 2.0 to 2.5). Soluble salts of bivalent (Mg, Co, Ni, Cu, Zn) or trivalent (Fe, In, La, Ce) metal ions were used. After the reaction mixtures were stirred overnight at 25 °C, the polyoxocations were precipitated with Na<sub>2</sub>SO<sub>4</sub> or Na<sub>2</sub>SeO<sub>4</sub> (at pH = 4.5). <sup>27</sup>Al NMR of these solutions, before precipitation, showed no evidence of new Al species. Only the spectra of M = Co<sup>2+</sup> and Cu<sup>2+</sup> were different, since little or no monomeric [Al(H<sub>2</sub>O)<sub>6</sub>]<sup>3+</sup> was detected. These paramagnetic ions apparently interact strongly with free Al<sup>3+</sup> ions.

The precipitates were characterized by powder XRD and <sup>27</sup>Al MAS NMR. There was no evidence of M incorporation. Only Al<sub>13</sub> was found. The XRD patterns are indexable in the cubic *F* $\bar{4}3m$  space group, with the unit cell parameter reported in Table

- (21) (a) Parker, W. O., Jr.; Kiricsi, I. *Appl. Catal.* **1995**, *21*, L7. (b) Nagy, J. B.; Bertrand, J.-C.; Palinko, I.; Kiricsi, I. *J. Chem. Soc., Chem. Commun.* **1995**, 2269. (c) Nagy, J. B.; Bertrand, J.-C.; Palinko, I.; Kiricsi, I. Presented at the 11<sup>th</sup> Zeolite Conference, Seoul, Korea, 1996. (d) Palinko, I.; Lazar, K.; Hannus, I.; Kiricsi, I. *J. Phys. Chem. Solids* **1996**, *57*, 1067. (e) Kiricsi, I.; Molnar, A.; Palinko, I.; Lazar, K. In *Catalysis by Microporous Materials*; Beyer, H. K., Karge, H. G., Kiricsi, I., Nagy, J. B., Eds.; Elsevier: Amsterdam, 1995; Vol. 94, p 63.
- (22) Bradley, S. M.; Kydd, R. A. *Catal. Lett.* **1991**, *8*, 185.
- (23) Espinosa, J.; Gomez, S.; Fuentes, G. A. *Zeolites and Related Microporous Materials. Stud. Surf. Sci. Catal.* **1994**, *84*, 283.

- (24) Sheldrick, G. M. *SHELX. A Program for Crystal Structure Determination*; Univ. of Cambridge: England, 1976.
- (25) Nardelli, M. *Comput. Chem.* **1983**, *7*, 95.
- (26) Kirkpatrick, R. J.; Phillips, B. L. *Appl. Magn. Reson.* **1993**, *4*, 213.
- (27) Johansson, G. *Acta Chem. Scand.* **1960**, *14*, 771.

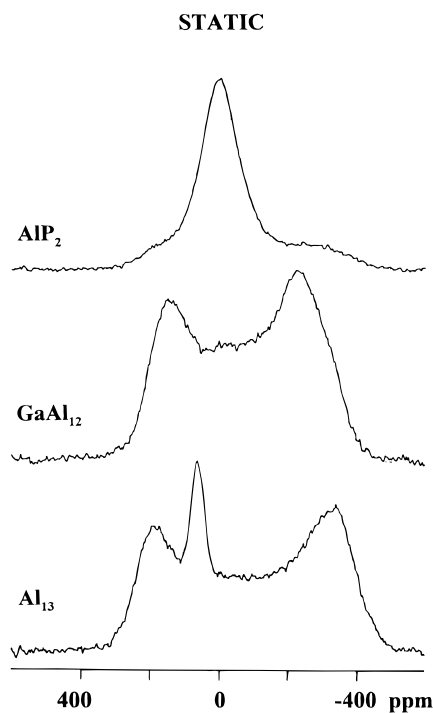


**Figure 1.** Solid state  $^{27}\text{Al}$  static NMR spectra of authentic  $\text{Al}_{13}$  sulfate, authentic  $\text{GaAl}_{12}$  sulfate, and  $\text{AlP}_2$  sulfate.

**Table 1.** Unit Cell Parameter for  $\text{Al}_{13}$  Salts Precipitated from Al + M Solutions

sample	$a$ (Å)	sample	$a$ (Å)
$\text{Al}_{13}\text{-SeO}_4$	18.067(6)	$\text{Al}_{13}\text{-SeO}_4 + \text{Zn}$	18.070(8)
$\text{Al}_{13}\text{-SeO}_4 + \text{Cu}$	18.067(7)	$\text{Al}_{13}\text{-SeO}_4 + \text{La}$	18.074(5)
$\text{Al}_{13}\text{-SeO}_4 + \text{Ni}$	18.064(7)	$\text{Al}_{13}\text{-SeO}_4 + \text{Ce}$	18.068(6)
$\text{Al}_{13}\text{-SeO}_4 + \text{Mg}$	18.061(6)	$\text{Al}_{13}\text{-SO}_4 + \text{La}$	17.856(6)
$\text{Al}_{13}\text{-SeO}_4 + \text{Co}$	18.059(8)	$\text{Al}_{13}\text{-SO}_4 + \text{Ga}$	17.859(5)

1. This is well-known for the selenate salt of  $\text{Al}_{13}$ <sup>27</sup> but is unprecedented for the sulfate salt. In fact, different polymorphic structures of the sulfate salt can be obtained, depending on solution pH. Normally, it tends to crystallize in the monoclinic  $P2/n$  ( $Pn$ ) or  $P2/a$  ( $Pa$ ) space groups, but tetrahedral crystals may be obtained with the cubic  $P4_232$  space group. Under our conditions (and in the presence of  $\text{La}^{3+}$  ions) the sulfate salt of  $\text{Al}_{13}$  crystallized as large tetrahedral crystals in the cubic  $F\bar{4}3m$  space group with  $a = 17.856(6)$  Å, isostructural with the selenate salt. Single-crystal XRD of this material (see below) was made to allow a direct structural comparison with other metal-substituted  $\text{Al}_{13}$  compounds.

Solid state  $^{27}\text{Al}$  NMR spectra of authentic  $\text{Al}_{13}$  (sulfate salt examined by single-crystal XRD) were obtained with the highest field available to us, both static (Figure 1) and with MAS (Figure 2) at the highest spin rates possible. The highly symmetrical  $T_d\text{-Al}$  of  $\text{Al}_{13}$  (QCC = 1.2(1) MHz, Table 2) gives a sharp signal near 63 ppm, even under modest NMR conditions.<sup>28</sup> This sharp signal readily distinguishes  $\text{Al}_{13}$  from other clusters, although broad  $T_d\text{-Al}$  signals are sometimes mistakenly assigned to  $\text{Al}_{13}$ .<sup>14,16,29</sup> Our 7 T field strength and 6.5 kHz MAS rate (Figure 2) cannot fully detect the 12  $O_h\text{-Al}$  nuclei of  $\text{Al}_{13}$ , since they have highly distorted coordination symmetries and thus large QCCs.<sup>2,28,30</sup> A QCC of 10.7(1) MHz (Table 2) was obtained from the static spectrum in Figure 1. The large second-order

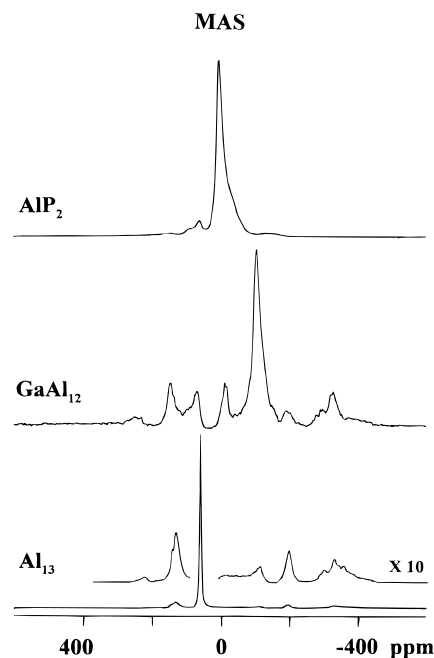


**Figure 2.** Solid state  $^{27}\text{Al}$  MAS NMR spectra (power mode) of authentic  $\text{Al}_{13}$  sulfate,  $\text{GaAl}_{12}$  sulfate, and  $\text{AlP}_2$  sulfate. Spin rate = 6.5 kHz.

**Table 2.** Isotropic Chemical Shifts ( $\delta$ ), Quadrupolar Coupling Constants (QCC), and Asymmetry Parameters ( $\eta$ ) Calculated by Computer Simulation of Solid State  $^{27}\text{Al}$  NMR Spectra for Sulfate Salts of  $\text{Al}_{13}$ ,  $\text{GaAl}_{12}$ , and  $\text{AlP}_2$

		$T_d\text{-Al}$			$O_h\text{-Al}$			ref
		$\delta$ (ppm)	QCC (MHz)	$\eta$	$\delta$ (ppm)	QCC (MHz)	$\eta$	
$\text{Al}_{13}$	static	70	$a$	0.6	7	10.7	0.1	$b$
	MAS	64	1.2	1				$b$
	MAS	63	0.8		8	10.2	0.2	$c$
$\text{GaAl}_{12}$	static				11	9.6	0.2	$b$
	static				18.3	4.2	0.6	$b$
$\text{AlP}_2$	static							$b$
	MAS	70	2.2	0		5	0	$d$

<sup>a</sup> Value of 2.6 MHz is found, but this reflects a large dipolar interaction as well. <sup>b</sup> This work, made with WinFit (Bruker) line shape analysis program. Error in fit is  $\pm 10\%$  of the value shown. <sup>c</sup> Reference 28, QCC of  $T_d\text{-Al}$  (error  $\pm 25\%$ ) from the field dependence of the chemical shift; QCC of  $O_h\text{-Al}$  (error =  $\pm 5\%$ ) from simulated static line shape. <sup>d</sup> Reference 18, QCC of  $T_d\text{-Al}$  from the field dependence of the chemical shift; QCC of  $O_h\text{-Al}$  estimated from the ratio of solution state line widths.

quadrupolar effect gives a broad signal for these  $O_h\text{-Al}$  (ca. 800 ppm) modulated by spinning sidebands. This MAS spectrum (Figure 2), although it represents only a small part of the  $O_h\text{-Al}$  nuclei, will be used here as a “fingerprint” to detect eventual modifications of  $O_h\text{-Al}$  nuclei in  $\text{Al}_{13}$ .

**Attempted Synthesis of  $\text{Al}_{13}$  Hybrids at 80 °C.** All substitution attempts were made directly by partially hydrolyzing ( $\text{OH}/(\text{Al} + \text{M}) = 2.25$ ) mixed aqueous solutions of  $\text{AlCl}_3$  and  $\text{MCl}_3$  (or  $\text{NO}_3$ ) ( $\text{Al}/\text{M} = 12$  and total concentration = 0.25 mol  $\text{L}^{-1}$ ). The aging kinetics was followed by solution state  $^{27}\text{Al}$  NMR, via the sharp  $T_d\text{-Al}$  signal intensity of  $\text{Al}_{13}$  (63 ppm), until all samples contained little or no  $\text{Al}_{13}$  (ca. 48 h). Since the amount of NMR-silent species actually decreases slightly with time for the solutions shown in Figure 3,  $\text{Al}_{13}$  disappearance is not attributed to Al sol formation. Thus, Keggin hybrid formation ( $\text{MAI}_{12}$  or  $\text{M}_{13}$ ) might occur in cases where  $\text{Al}_{13}$  decay (at 80 °C) is faster than that known for  $\text{AlP}_2$  formation. However, both substitution of the central  $T_d\text{-Al}$  of  $\text{Al}_{13}$  and polymerization of  $\text{Al}_{13}$  units (to form  $\text{AlP}_2$  or higher species) cause the loss of the 63 ppm signal. Only analysis of the solid

(28) Kunwar, A. C.; Thompson, A. R.; Gutowsky, H. S.; Oldfield, E. J. *Magn. Reson.* **1984**, *60*, 467.

(29) (a) Jones, D. J.; Leloup, J.-M.; Ding, Y.; Roziere, J. *Solid State Ionics* **1993**, *61*, 117. (b) Hernando, M. J.; Pesquera, C.; Benito, I.; Gonzalez, F. *Chem. Mater.* **1996**, *8*, 76.

(30) Tennakoon, D. T. B.; Jones, W.; Thomas, J. M. *J. Chem. Soc., Faraday Trans. 1* **1986**, *82*, 3081.

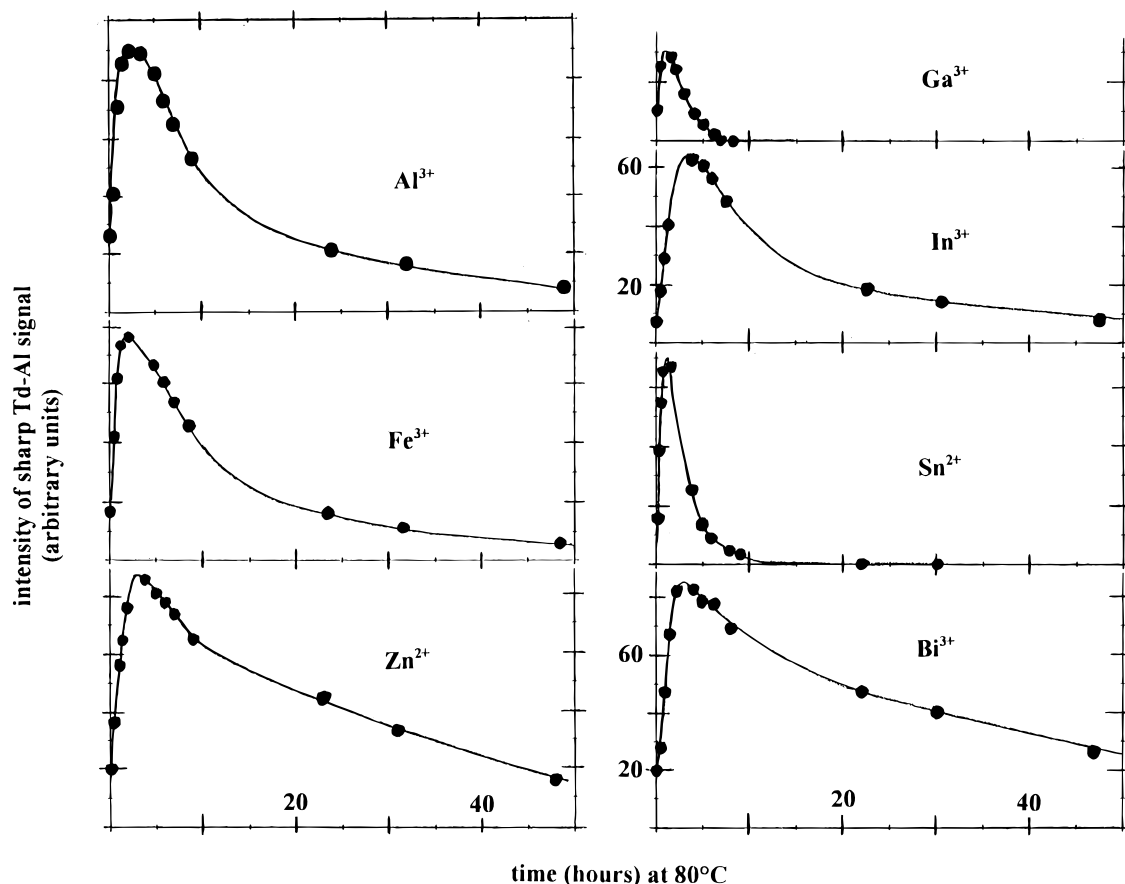


**Figure 3.** 80 °C aging profiles showing the formation and disappearance of  $\text{Al}_{13}$  as monitored (at 25 °C) by the intensity of the sharp  $T_d$ -Al NMR resonance at 63 ppm.

**Table 3.** Apparent First-Order Rate Constants ( $k_{\text{app}}$ ) for Disappearance of  $\text{Al}_{13}$  During Aging of Partially Hydrolyzed Al + M (12:1 Mole Ratio) Solutions at 80 °C (Starting Aqueous  $\text{AlCl}_3$  Concentration = 0.25 mol  $\text{L}^{-1}$ )

M(aq)	$k_{\text{app}} (\times 10^2 \text{ h}^{-1})^a$	M(aq)	$k_{\text{app}} (\times 10^2 \text{ h}^{-1})^a$
$\text{AlCl}_3$	4.8(8)	$\text{In}(\text{NO}_3)_3$	4.8
$\text{FeCl}_3$	5.8	$\text{SnCl}_2$	38
$\text{ZnCl}_2$	3.7	$\text{La}(\text{NO}_3)_3$	4.1
$\text{Ga}(\text{NO}_3)_3$	54	$\text{Bi}(\text{NO}_3)_3$	2.6

<sup>a</sup> Error margin estimated to be  $\pm 15\%$  of the value given.

product (XRD, NMR), obtained by precipitation, can permit a distinction between substitution (with M) and conversion (to  $\text{AlP}_2$  or other species).

Aging of freshly hydrolyzed  $\text{AlCl}_3$  at 80 °C, under our reproducible conditions,<sup>21a</sup> causes  $\text{Al}_{13}$  to be converted to  $\text{AlP}_2$  with an apparent first-order rate constant of  $4.8(8) \times 10^{-2} \text{ h}^{-1}$ . This is slightly faster than the rate ( $0.036 \text{ h}^{-1}$ ) observed by Nazar and co-workers<sup>17</sup> for a “pure”  $\text{Al}_{13}$  solution ( $0.035 \text{ mol L}^{-1}$ ) aged at 85 °C. Unlike our solutions, which contain all of the hydrolysis products (even NMR-silent Al sol), their solutions contained only  $\text{Al}_{13}$ .

The time course for  $\text{Al}_{13}$  formation and the subsequent decay during 80 °C aging of the freshly hydrolyzed Al + M solutions is shown in Figure 3 along with that for  $\text{AlCl}_3$ . The profiles for M =  $\text{La}^{3+}$  (not shown) and most of the M shown are the same as that observed for  $\text{AlCl}_3$ .  $\text{Al}_{13}$  decay rates are given in Table 3. Only the M =  $\text{Ga}^{3+}$  and  $\text{Sn}^{2+}$  solutions exhibited a faster conversion than that for the pure  $\text{AlCl}_3$  solution. The presence of  $\text{Bi}^{3+}$  slightly retards conversion.

The solutions with M =  $\text{Ga}^{3+}$  and  $\text{La}^{3+}$  were also examined by  $^{71}\text{Ga}$  and  $^{139}\text{La}$  NMR, respectively. In the case of M =  $\text{Ga}^{3+}$ , initially there is competition for polyoxocation formation.  $\text{Al}_{13}$  and  $\text{GaAl}_{12}$  form simultaneously, as seen (Figure 4) by the

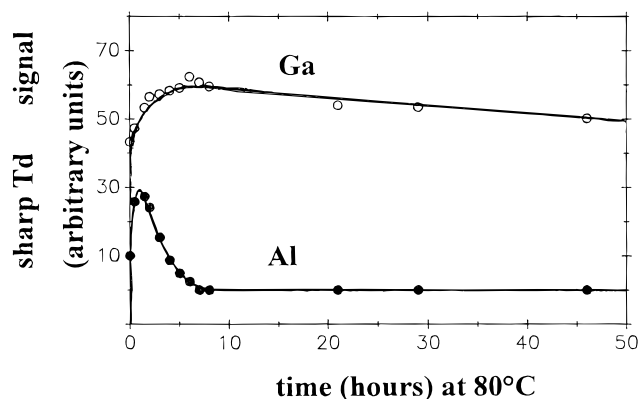


**Figure 4.** 80 °C aging profiles showing the intensity variations of the sharp  $^{27}\text{Al}$  and  $^{71}\text{Ga}$  NMR resonances of  $T_d$ -Al (63 ppm) and  $T_d$ -Ga (137 ppm) with time, for the M =  $\text{Ga}^{3+}$  solution.

increase in the sharp  $T_d$ -Al resonance of  $\text{Al}_{13}$  (63 ppm) and the sharp  $T_d$ -Ga of  $\text{GaAl}_{12}$  (137 ppm). Within 7 h at 80 °C, all of the  $\text{Al}_{13}$  was converted to the more stable Ga hybrid, with no  $\text{AlP}_2$  formation evident. Slow decay of  $\text{GaAl}_{12}$  also occurred. No changes in the  $^{139}\text{La}$  NMR spectra (shift = 6.9 ppm or area) were observed during the aging of the M =  $\text{La}^{3+}$  solution. This (and the other observations) confirms that no La incorporation occurs. Substitution with  $\text{La}^{3+}$  was also attempted under reflux conditions.  $\text{AlP}_2$  and  $\text{La}_2(\text{SO}_4)_3$  were the sole products, of the precipitated salts, as evidenced by NMR ( $^{27}\text{Al}$ ,  $^{139}\text{La}$ ).

$\text{AlP}_2$ <sup>17,18</sup> was obtained by refluxing hydrolyzed  $\text{AlCl}_3$  ( $\text{OH}/\text{Al} = 2.25$ ) for 2 days, until complete disappearance of  $\text{Al}_{13}$ . The  $^{27}\text{Al}$  MAS NMR spectrum (Figure 2) contains a broad  $T_d$ -Al and a relatively sharp  $O_h$ -Al signal, with observed shifts of 60 and 4 ppm, respectively. Clearly, the  $O_h$ -Al of  $\text{AlP}_2$  have higher symmetry (smaller QCC) than those of  $\text{Al}_{13}$ , since a

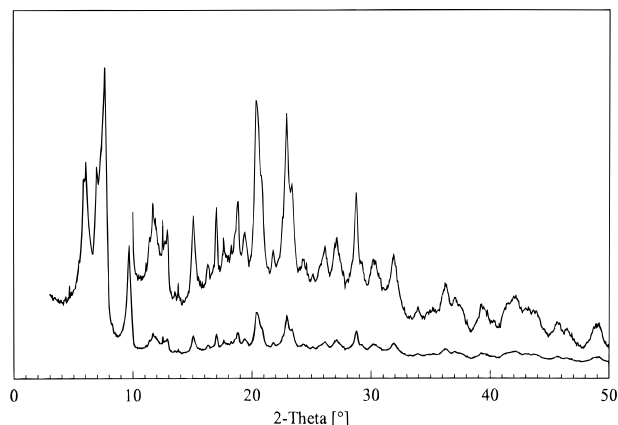


Figure 5. Powder XRD pattern of AlP<sub>2</sub> sulfate.

signal resembling the central transition is seen in the MAS spectrum (Figure 2). Calculation of QCCs for static spectra confirm this (Table 2). Also, visual comparison of the static spectra of the two clusters (Figure 1) reveals the  $T_d$ -Al of AlP<sub>2</sub> to be much less symmetrical than that of Al<sub>13</sub>.<sup>18</sup> In Figure 2, the  $T_d$ -Al signal of AlP<sub>2</sub> is broader than that of  $O_h$ -Al. This is contrary to the findings of Nazar et al. (Table 2, ref 18), which is not readily explained by their use of a higher magnetic field strength. Perhaps exchange phenomena are important. Thus, AlP<sub>2</sub> (or similar species with higher molecular weight, e.g., AlP<sub>3</sub>) as synthesized here is not exactly the same as that prepared by others.<sup>18</sup> However, we will refer to our product as AlP<sub>2</sub>, even though it apparently contains small amounts of other polymeric hydroxides.

The powder XRD pattern of AlP<sub>2</sub> is shown in Figure 5. It is a rather complex pattern that reveals the presence of a significant amount of amorphous material, together with the AlP<sub>2</sub> crystalline phase. All of the attempted substitutions gave powdered precipitates with XRD patterns similar to that of AlP<sub>2</sub> except for Ga<sup>3+</sup>, which gave the pattern for cubic GaAl<sub>12</sub>-SO<sub>4</sub>.

Solid state NMR shows that after 2 days at 80 °C all of the solutions contained mainly AlP<sub>2</sub>, except for M = Ga<sup>3+</sup>. Complete conversion to AlP<sub>2</sub> occurred only for M = Sn<sup>2+</sup>. This metal ion apparently enhances the condensation of Al<sub>13</sub>, perhaps by chemically linking Al<sub>12</sub> units. Solid state <sup>27</sup>Al NMR spectra of authentic GaAl<sub>12</sub> (determined by single-crystal XRD) are shown in Figures 1 and 2. The  $O_h$ -Al signals exhibit large quadrupolar broadening effects similar to those of Al<sub>13</sub> (Table 2) and give a distinct MAS signal pattern with a prominent modulated side band at -100 ppm under our conditions. This spectrum is more highly resolved at a 9.4 T field strength<sup>2</sup> as second-order quadrupolar effects are reduced.

**Single-Crystal Structural Analysis.** Single-crystal structural analysis was performed on Al<sub>13</sub> sulfate, obtained by slow crystallization of the solution containing La<sup>3+</sup> ions treated at 25 °C, and on GaAl<sub>12</sub> sulfate, obtained from the solution containing Ga<sup>3+</sup> ions treated at 80 °C. These two structures, both of cubic cell symmetry, provide the first rigorous comparison between these two polyoxocations since, for the first time, crystals of the sulfate salt of Al<sub>13</sub> were obtained. Emphasis was placed on verifying if the geometrical considerations can justify the higher thermal stability of GaAl<sub>12</sub>, as suggested by others.<sup>2,3</sup> The main crystallographic data are reported in Table 4, selected geometrical data in Table 5. To facilitate the comparison with previously published crystallographic data of the cubic selenate salt of Al<sub>13</sub><sup>27</sup> and of the cubic sulfate salt of GaAl<sub>12</sub>,<sup>4</sup> we have maintained the same atom-labeling scheme.

Incorporation of Ga produces an expansion of the central tetrahedron, with the four Ga–O(2) bond lengths of 1.879(5) Å being slightly smaller than those found by Goerz et al. (1.892-

Table 4. Crystallographic Data for Al<sub>13</sub> and GaAl<sub>12</sub> Sulfate Salts

	Na[AlO <sub>4</sub> Al <sub>12</sub> (OH) <sub>24</sub> ·(H <sub>2</sub> O) <sub>12</sub> ](SO <sub>4</sub> ) <sub>2</sub> ·10H <sub>2</sub> O	Na[GaO <sub>4</sub> Al <sub>12</sub> (OH) <sub>24</sub> ·(H <sub>2</sub> O) <sub>12</sub> ](SO <sub>4</sub> ) <sub>2</sub> ·10H <sub>2</sub> O
fw	1626.49	1669.23
space group	<i>F</i> 43 <i>m</i> (No. 216)	<i>F</i> 43 <i>m</i> (No. 216)
<i>a</i> (Å)	17.856(2)	17.869(3)
<i>V</i> (Å <sup>3</sup> )	5693.2(11)	5705.6(17)
<i>Z</i>	4.00	4.00
<i>T</i> (°C)	25.00	25.00
radiation, λ (Å)	Mo Kα, 0.710 69	Mo Kα, 0.710 69
ρ <sub>calcd</sub> (g cm <sup>-3</sup> )	1.898	1.943
μ (cm <sup>-1</sup> )	5.025	9.473
<i>R</i> <sup>a</sup>	0.058	0.055
<i>R</i> <sub>w</sub> <sup>b</sup>	0.064	0.059

$$^a R = \sum(|F_o - F_c|)/\sum|F_o|. \quad ^b R_w = [\sum w(|F_o - F_c|)^2/\sum w|F_o|^2]^{1/2}.$$

Table 5. Selected Geometrical Data for Al<sub>13</sub> and GaAl<sub>12</sub> Sulfate Salts

	M <sub>T</sub> = Al	M <sub>T</sub> = Ga
M <sub>T</sub> -O(2) × 4	1.831(4)	1.879(5)
Al <sub>o</sub> -O(1) × 2	1.857(6)	1.852(6)
Al <sub>o</sub> -O(2)	2.026(4)	2.009(6)
Al <sub>o</sub> -O(3)	1.961(4)	1.962(6)
Al <sub>o</sub> -O(4) × 2	1.857(6)	1.869(7)
O(2)-M <sub>T</sub> -O(2') × 6	109.5(2)	109.5(2)
O(1)-Al <sub>o</sub> -O(1')	78.0(2)	77.5(2)
O(1)-Al <sub>o</sub> -O(2) × 2	95.4(2)	95.3(2)
O(1)-Al <sub>o</sub> -O(3) × 2	92.3(2)	92.7(2)
O(1)-Al <sub>o</sub> -O(4) × 2	94.2(2)	94.5(2)
O(1)-Al <sub>o</sub> -O(4') × 2	171.6(2)	171.1(3)
O(2)-Al <sub>o</sub> -O(3)	170.1(2)	169.6(3)
O(2)-Al <sub>o</sub> -O(4) × 2	82.0(2)	81.5(2)
O(3)-Al <sub>o</sub> -O(4) × 2	91.3(2)	91.4(2)
O(4)-Al <sub>o</sub> -O(4')	93.3(2)	93.2(2)
Al <sub>o</sub> -O(1)-Al <sub>o</sub> '	101.4(2)	102.1(3)
Al <sub>o</sub> -O(2)-M <sub>T</sub> × 3	123.6(2)	122.6(3)
Al <sub>o</sub> -O(2)-Al <sub>o</sub> ' × 3	92.3(2)	93.7(2)
Al <sub>o</sub> -O(4)-Al <sub>o</sub> '	103.7(2)	103.3(3)

(6) Å) and significantly longer than the typical tetrahedral Ga–O bond distance (e.g., 1.82 Å in β-Ga<sub>2</sub>O<sub>3</sub>). However, in spite of the larger dimension of the central tetrahedral atom, the geometries of the surrounding octahedra are almost unaffected (Table 5). In fact, the increase of the M<sub>T</sub>-O(2) distance produces a contraction of the Al<sub>o</sub>-O(2) bond from 2.026(4) to 2.009(6) Å, while no significant differences exist among the bond angles of the two polyoxocations, which generally agree within the standard deviations.

## Conclusions

Metal ion substitution of Al in Al<sub>13</sub> was attempted using Mg<sup>2+</sup>, Fe<sup>3+</sup>, Co<sup>2+</sup>, Ni<sup>2+</sup>, Cu<sup>2+</sup>, Zn<sup>2+</sup>, In<sup>3+</sup>, La<sup>3+</sup>, and Ce<sup>3+</sup> at 25 °C and using Fe<sup>3+</sup>, Zn<sup>2+</sup>, Ga<sup>3+</sup>, In<sup>3+</sup>, Sn<sup>2+</sup>, La<sup>3+</sup>, and Bi<sup>3+</sup> at 80 °C. Only the GaAl<sub>12</sub> hybrid was evidenced by NMR and XRD methods under our experimental conditions. Metal ion substitutions of Al<sub>13</sub> that are claimed in the literature frequently involve the modification of condensed Al<sub>13</sub> clusters (AlP<sub>2</sub>-type species) or polymeric hydroxides, not Al<sub>13</sub>. The higher thermal stability of GaAl<sub>12</sub> (compared to Al<sub>13</sub>), observed both in solution and in PILCs, cannot be justified from the structural considerations of the solid polyoxocations. This conclusion was possible, for the first time, by comparison of the single-crystal XRD data for the isostructural forms (cubic symmetry) of these two polyoxocations.

**Supporting Information Available:** Listings of crystallographic data and tables of positional and anisotropic thermal parameters for Al<sub>13</sub> and GaAl<sub>12</sub> sulfate salts (6 pages). Ordering information is given on any current masthead page.